

PAPER

Pilot-Aided Adaptive Prediction Channel Estimation in a Frequency-Nonselective Fading Channel

Shinsuke TAKAOKA[†], *Student Member and* Fumiyuki ADACHI[†], *Regular Member*

SUMMARY Pilot-aided adaptive prediction channel estimation is proposed for coherent detection in a frequency-nonselective fading channel. It is an extension of the conventional weighted multi-slot averaging (WMSA) channel estimation and consists of 3 steps. A block of N_p pilot symbols is periodically transmitted, each pilot block being followed by N_d data symbols to form a data slot. In the first step, the instantaneous channel gain is estimated by coherent addition of N_p pilot symbols. Using the K past and K future estimated instantaneous channel gains, the second step predicts the instantaneous channel gains at the end and beginning of data slot of interest by a forward predictor and a backward predictor, respectively. The tap-weights of forward prediction and backward prediction are adaptively updated using the normalized least mean square (NLMS) algorithm. Finally, in the third step, the instantaneous channel gain at each data symbol position within the data slot of interest is estimated by simple averaging or linear interpolation using the two adaptively predicted instantaneous channel gains. The computer simulation confirms that the proposed adaptive prediction channel estimation achieves better bit error rate (BER) performance than the conventional WMSA channel estimation in a fast fading channel and/or in the presence of frequency offset between a transmitter and a receiver.

key words: fading channel, channel estimation, pilot symbol, adaptive prediction, normalized LMS

1. Introduction

In mobile radio, multipath fading is produced by reflection and diffraction of the transmitted signal by many obstacles between a transmitter and a receiver; the received signal amplitude and phase fluctuate in a random manner [1]. Coherent detection requires channel estimation, which, however, is difficult to achieve in a fast fading channel, and thus the bit error rate (BER) performance degrades. To perform coherent detection in a fast fading channel, pilot-aided channel estimation was proposed [2], [3]. In a fast fading channel, the channel gain varies rapidly. In order to cope with fast fading, first and second order interpolation methods could be used [2], [4]. However, transmission of many pilot symbols leads to significant power loss. Recently, weighted multi-slot averaging (WMSA) channel estimation was proposed for a direct sequence code division multiple access (DS-CDMA) mobile radio [5]. The WMSA channel estimation consists of the following two steps. A

block of N_p pilot symbols is transmitted, each pilot block being followed by N_d data symbols to form a data slot. In the first step, the instantaneous channel gain is estimated by coherent addition of N_p pilot symbols. Then, at the second step, the $2K$ instantaneous channel gains are input to a $2K$ -tap filter to estimate the channel gain at each data symbol position within the data slot of interest. In [5], the tap-weights are optimized based on computer simulations. $K = 1$ WMSA channel estimation uses simple average of the two consecutive pilot blocks [6]. However, using the time invariant tap-weights cannot always minimize the BER in changing fading environment due to user's movement. Then, adaptive methods of the tap-weights were proposed in [7], [8]. In the presence of the frequency offset between a transmitter and a receiver, the resultant phase rotation further degrades the BER performance. For reducing the adverse effect of frequency offset, a pilot-aided frequency offset compensation method was proposed in [9].

In this paper, a pilot-aided adaptive prediction channel estimation is proposed that performs coherent detection in the fast fading channel and/or in the presence of frequency offset. It is an extension of the conventional WMSA channel estimation and consists of 3 steps. In the first step, as in the conventional WMSA channel estimation, the instantaneous channel gain is estimated by coherent addition of N_p pilot symbols. The second step predicts the instantaneous channel gains at the end and beginning of data slot by a forward predictor and a backward predictor, respectively. The tap-weights are adaptively updated using the normalized least mean square (NLMS) algorithm [10]. Finally, in the third step, the instantaneous channel gain at each data symbol position within the data slot of interest is estimated by simple averaging or linear interpolation using the two adaptively predicted instantaneous channel gains.

The remainder of the paper is organized as follows. Section 2 presents the transmission system and Sect. 3 describes the proposed adaptive prediction channel estimation. In Sect. 4, the BER performance using the proposed adaptive prediction channel estimation is evaluated by computer simulation. The computer simulation confirms that the adaptive prediction channel estimation achieves better BER performance than the conventional non-adaptive WMSA channel estimation

Manuscript received October 24, 2001.

Manuscript revised March 7, 2002.

[†]The authors are with Electrical and Communication Engineering, Graduate School of Engineering, Tohoku University, Sendai-shi, 980-8579 Japan.

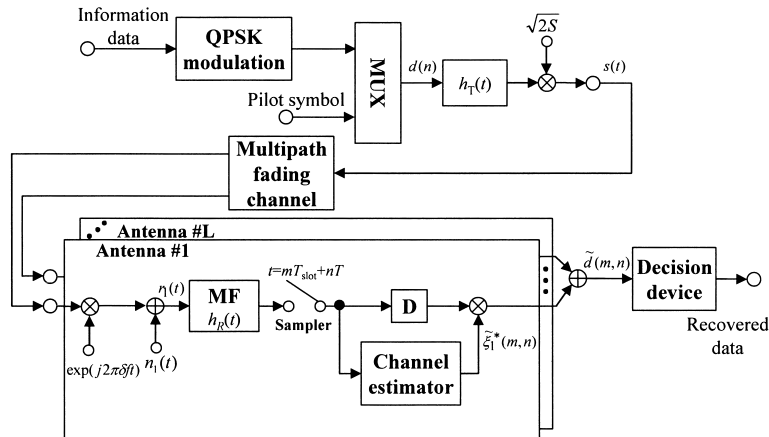


Fig. 1 Transmission system model.

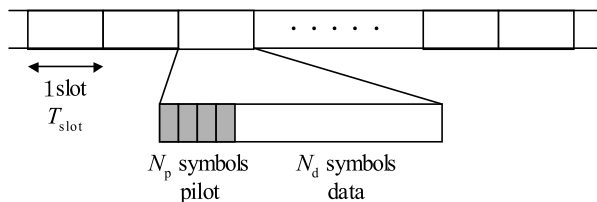


Fig. 2 Slot structure.

in the fast fading channel and/or in the presence of frequency offset. Section 5 concludes the paper.

2. Transmission System Model

A low-pass equivalent transmission system model is illustrated in Fig. 1. First, the binary data sequence to be transmitted is transformed into a sequence of quadrature phase shift keying (QPSK)-modulated symbols. The transmitted signal $s(t)$ in the complex representation can be expressed as

$$s(t) = \sqrt{2S} \sum_{n=-\infty}^{\infty} d(n)h_T(t - nT), \quad (1)$$

where S is the average transmit signal power, $d(n) = \exp(j\phi_n)$, $\phi_n = 0, \pi/2, \pi, 3\pi/2$, is the n th QPSK symbol with length T , and $h_T(t)$ is the transmit filter impulse response. As shown in Fig. 2, a block of N_p pilot symbols is placed at the beginning of each data slot and is followed by N_d data symbols. The slot length T_{slot} is given by $T_{slot} = (N_p + N_d)T$.

Transmitted signal is received via a fading channel. Without loss of generality, a frequency-nonspecific fading channel is assumed. Denoting the time varying complex channel gain seen on the l th ($l = 1, 2, \dots, L$) receive antenna by $\xi_l(t)$, the received signal can be expressed as

$$r_l(t) = s(t)\xi_l(t) \exp(j2\pi\delta ft) + n_l(t), \quad (2)$$

where δf is the frequency offset between the transmit-

ter and the receiver, $n_l(t)$ is the additive white Gaussian noise (AWGN) with a single sided power spectrum density of N_0 . It is assumed that the signal distortion, caused by the receive matched filter (MF) having the impulse response of $h_R(t) = (1/T)h_T(-t)$, due to the fading and the frequency offset can be neglected. In this paper, assuming ideal sampling timing, the MF output is sampled at the symbol rate. The MF output signal sample $r_l(m, n)$ on the l th antenna at the time position $t = mT_{slot} + nT$ of the n th symbol in the m th slot is expressed as

$$\begin{aligned} r_l(m, n) &= r_l(mT_{slot} + nT) \\ &= \sqrt{2S}d(m, n)\xi_l(m, n)f(m, n) + \rho_l(m, n), \end{aligned} \quad (3)$$

where,

$$\begin{aligned} d(m, n) &= d(m(N_p + N_d) + n), \\ \xi_l(m, n) &= \xi_l(mT_{slot} + nT), \\ f(m, n) &= \exp[j2\pi\delta f(mT_{slot} + nT)], \end{aligned}$$

and $\rho_l(m, n)$ is the noise component. Adaptive prediction channel estimation is performed using the sample sequence of $\{r_l(m, n)\}$ and the estimated channel gain is denoted by $\tilde{\xi}_l(m, n)$. The delay element “ D ” in Fig. 1 has a time delay of $D = KT_{slot}$ for the adaptive prediction channel estimation which is described in Sect. 3.

The maximal ratio combining (MRC) is assumed for antenna diversity reception. The MRC combiner output $\tilde{d}(m, n)$, which is the decision variable, is expressed as

$$\tilde{d}(m, n) = \sum_{l=1}^L r_l(m, n)\tilde{\xi}_l^*(m, n), \quad (4)$$

where L is the number of antennas and $*$ denotes the complex conjugate.

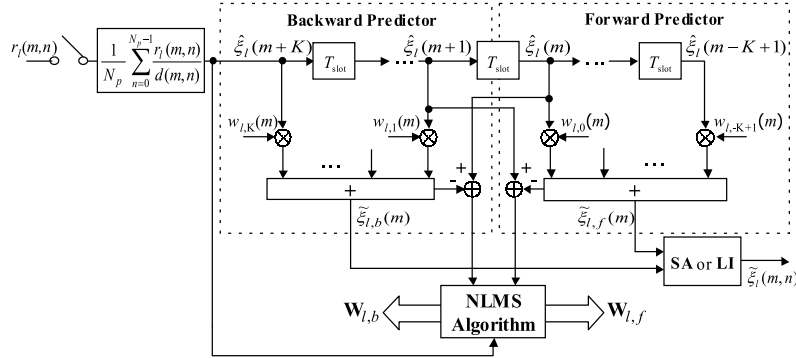


Fig. 3 Structure of pilot-aided adaptive prediction channel estimation.

3. Adaptive Prediction Channel Estimation

3.1 Principle of Operation

Figure 3 illustrates the structure of the adaptive prediction channel estimation, which consists of 3 steps. In the first step, the instantaneous channel gain is estimated by coherent addition of N_p received pilot symbols after removing pilot symbol phase. The instantaneous channel estimate $\hat{\xi}_l(m)$ at the beginning of the m th data slot is given by

$$\hat{\xi}_l(m) = \frac{1}{N_p} \sum_{n=0}^{N_p-1} \frac{r_l(m,n)}{d(m,n)}. \quad (5)$$

Then, the second step predicts the instantaneous channel gains, $\tilde{\xi}_{l,f}(m)$ and $\tilde{\xi}_{l,b}(m)$, at the end and the beginning of the m th data slot, by a forward predictor and a backward predictor, using the K past and K future estimated instantaneous channel gains, $\{\hat{\xi}_l(m+k)\}$, $k = -(K-1) \sim K$, respectively. The tap-weights of the forward predictor and a backward predictor are adaptively updated using the NLMS algorithm. $\tilde{\xi}_{l,f}(m)$ and $\tilde{\xi}_{l,b}(m)$ are given by

$$\begin{aligned} \tilde{\xi}_{l,f}(m) &= \sum_{k=-(K-1)}^0 w_{l,k}(m) \hat{\xi}_l(m+k) \\ &= \mathbf{W}_{l,f}(m) \mathbf{X}_{l,f}^T(m) \end{aligned} \quad (6a)$$

$$\begin{cases} \mathbf{W}_{l,f}(m) = \{w_{l,0}(m), w_{l,-1}(m), \\ \quad \dots, w_{l,-K+1}(m)\} \\ \mathbf{X}_{l,f}(m) = \{\hat{\xi}_l(m), \hat{\xi}_l(m-1), \\ \quad \dots, \hat{\xi}_l(m-K+1)\} \end{cases} \quad (6b)$$

$$\begin{aligned} \tilde{\xi}_{l,b}(m) &= \sum_{k=1}^K w_{l,k}(m) \hat{\xi}_l(m+k) \\ &= \mathbf{W}_{l,b}(m) \mathbf{X}_{l,b}^T(m) \end{aligned} \quad (7a)$$

$$\begin{cases} \mathbf{W}_{l,b}(m) = \{w_{l,1}(m), w_{l,2}(m), \\ \quad \dots, w_{l,K}(m)\} \\ \mathbf{X}_{l,b}(m) = \{\hat{\xi}_l(m+1), \hat{\xi}_l(m+2), \\ \quad \dots, \hat{\xi}_l(m+K)\} \end{cases} \quad (7b)$$

where $(\cdot)^T$ denotes transpose, $\mathbf{W}_{l,f}$ and $\mathbf{W}_{l,b}$ are respectively the complex tap-weight row vectors for the forward predictor and backward predictor, and $\mathbf{X}_{l,f}(m)$ and $\mathbf{X}_{l,b}(m)$ are respectively the row vectors of the estimated instantaneous channel gains to be used in the forward predictor and backward predictor.

Finally, in the third step, the instantaneous channel gain $\tilde{\xi}_l(m,n)$ at the n th data symbol position of the m th data slot is estimated by simple averaging (SA) or linear interpolation (LI) using the two adaptively predicted instantaneous channel gains, $\tilde{\xi}_{l,f}(m)$ and $\tilde{\xi}_{l,b}(m)$. $\tilde{\xi}_l(m,n)$ is given by

SA:

$$\tilde{\xi}_l(m,n) = \frac{\tilde{\xi}_{l,f}(m) + \tilde{\xi}_{l,b}(m)}{2} \quad (8a)$$

LI:

$$\begin{aligned} \tilde{\xi}_l(m,n) &= \frac{\left(n - \frac{N_p - 1}{2}\right)}{N_p + N_d} \tilde{\xi}_{l,f}(m) \\ &\quad + \left\{1 - \frac{\left(n - \frac{N_p - 1}{2}\right)}{N_p + N_d}\right\} \tilde{\xi}_{l,b}(m). \end{aligned} \quad (8b)$$

3.2 Tap-Weight Adaptation

After making decisions on all data symbols of the m th data slot, the NLMS algorithm updates the tap-weight vectors, $\mathbf{W}_{l,f}$ and $\mathbf{W}_{l,b}$, using $\hat{\xi}_l(m+1)$ and $\hat{\xi}_l(m)$ as the reference signals:

$$\left\{ \begin{array}{l} \mathbf{W}_{l,f}(m+1) = \mathbf{W}_{l,f}(m) \\ + \mu \frac{e_{l,f}(m)}{\sum_{j=-(K-1)}^0 |\hat{\xi}_l(m+j)|^2} \mathbf{X}_{l,f}^*(m) \\ e_{l,f}(m) = \hat{\xi}_l(m+1) - \tilde{\xi}_{l,f}(m) \end{array} \right. \quad (9a)$$

$$\left\{ \begin{array}{l} \mathbf{W}_{l,b}(m+1) = \mathbf{W}_{l,b}(m) \\ + \mu \frac{e_{l,b}(m)}{\sum_{j=1}^K |\hat{\xi}_l(m+j)|^2} \mathbf{X}_{l,b}^*(m) \\ e_{l,b}(m) = \hat{\xi}_l(m) - \tilde{\xi}_{l,b}(m) \end{array} \right. , \quad (9b)$$

where $e_{l,f}(m)$ and $e_{l,b}(m)$ are the estimation errors and μ is the step size.

The major cause of errors is the AWGN in a slow fading channel, however, it is the random phase noise (sometimes called as the random FM noise) in a fast fading channel. The tap-weight adaptation for forward prediction and backward prediction use the instantaneous channel estimates of one slot future and one slot past as the reference signals, respectively (see Eq. (9)). Therefore, while the proposed adaptive prediction channel estimation acts as the prediction filter in a fast fading channel, it acts as an averaging filter, i.e., the tap-weights become almost the same, to minimize the effect of the AWGN in a slow fading channel.

4. Computer Simulation

We assume QPSK modulation and a frequency-nonselctive Rayleigh fading channel with $L = 2$ MRC diversity reception. (Although QPSK modulation is assumed in this paper, the proposed adaptive prediction channel estimation can also be applied to other high-level modulation schemes, e.g., 16 quadrature amplitude modulation (16QAM).) Since channel estimation accuracy depends on the value of N_p , the selection of N_p is an important issue. As N_p increases, the signal-to-noise ratio (SNR) of the instantaneous channel estimate $\hat{\xi}_l(m)$ in Eq. (5) improves due to coherent addition of N_p received pilot symbols, leading to the improved SNR of $\tilde{\xi}_{l,f}(m)$ and $\tilde{\xi}_{l,b}(m)$. Accordingly, the BER performance improves. From the computer simulations performed to evaluate the achievable BER performance for various values of N_p in a slow fading environment we found that as N_p increases from $N_p = 1$ to 2 and further, to 3, the BER performance improves, but the additional performance improvement becomes quite small for N_p larger than 4. On the other hand, the power loss due to the transmission of non-information bearing pilot symbols increases. Hence, in the following computer simulations, we set $N_p = 4$ and $N_d = 60$. For comparison, the conventional non-adaptive WMSA

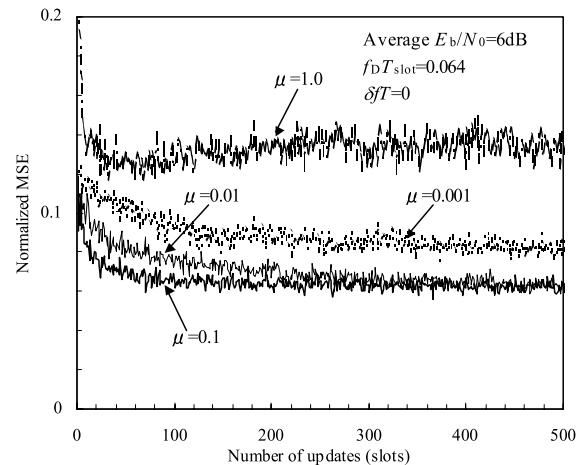


Fig. 4 Tap-weight convergence rate of a $K = 4$ adaptive prediction channel estimation.

channel estimation using $K = 1, 2,$ and 3 are also assumed: the tap-weight vectors for $K = 1, 2$ and 3 are $\{1.0, 1.0\}$, $\{0.6, 1.0, 1.0, 0.6\}$ and $\{0.3, 0.8, 1.0, 1.0, 0.8, 0.3\}$, respectively [5].

4.1 Tap-Weight Convergence

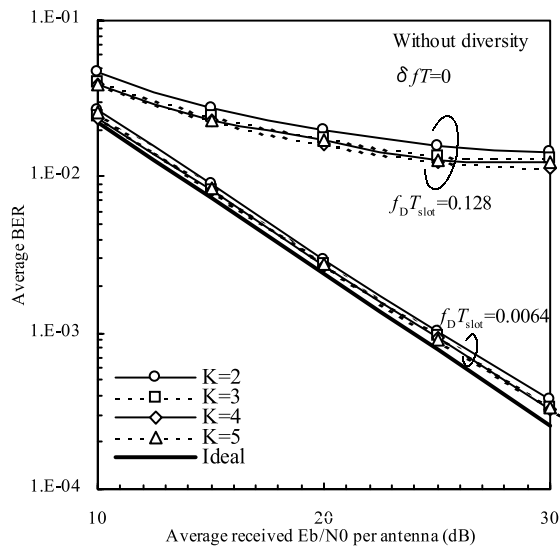
As the step size μ becomes larger, the tap-weight convergence rate becomes faster, but the prediction error becomes larger. The normalized mean square error (MSE) was obtained by taking ensemble average of the squared value of prediction error $e_{l,f}(m)$ over 800 independent trials and for varying m . Figure 4 plots the normalized MSE of a $K = 4$ adaptive prediction channel estimation as a function of number of updates (number of elapsed slots from the beginning) for the normalized maximum fading Doppler frequency $f_d T_{slot} = 0.064$, the average received signal energy per bit-to-AWGN power spectrum density ratio $E_b/N_0 = 6$ dB, and no frequency offset $\delta f = 0$. The initial tap-weight vectors, $\mathbf{W}_{l,f}$ and $\mathbf{W}_{l,b}$, were set as $[1.0, 0, 0, 0]$ and $[1.0, 0, 0, 0]$, respectively. This means that the adaptive prediction channel estimation starts with the $K = 1$ WMSA channel estimation. The use of larger μ provides faster convergence, but the achievable MSE becomes larger when the tap-weights have converged (after around more than 300 updates (or slots)). As is expected, when $\mu = 1.0$, faster convergence but with larger MSE is observed. On the other hand, when $\mu = 10^{-3}$, the tap weight convergence rate is too slow. It can be seen from Fig. 4 that the achievable MSE is almost the same for $\mu = 0.1$ and 0.01 . Hence, $\mu = 0.1$ is considered to provide overall best property of fast convergence and small MSE, and was assumed in the following simulations.

4.2 Influence of Number of Taps

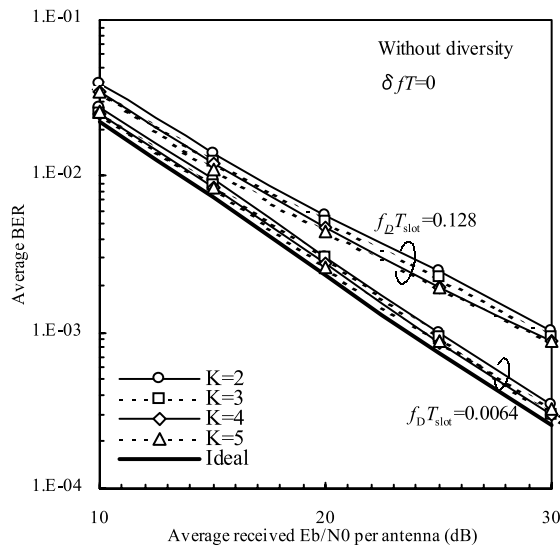
The BER performance is plotted with the number $2K$

of estimation filter taps as a parameter in Fig. 5(a) and Fig. 5(b) when the 3rd step uses simple averaging filter and linear interpolation filter, respectively. No antenna diversity was assumed. For comparison, the BER performance with ideal channel estimation (and *no pilot transmission*) is also plotted. The theoretical BER $P_e(\Gamma)$ for QPSK can be given by [11]

$$P_e(\Gamma) = \begin{cases} \frac{1}{2} \left(1 - \sqrt{\frac{\Gamma}{1+\Gamma}} \right), & L = 1 \\ \frac{1}{2} \left(1 - \frac{1 + \frac{3}{2\Gamma}}{\left(1 + \frac{1}{\Gamma}\right)^{\frac{3}{2}}} \right), & L = 2 \end{cases}, \quad (10)$$



(a) Simple averaging (SA) filter in the 3rd step



(b) Linear interpolation (LI) filter in the 3rd step

Fig. 5 Influence of number of taps in adaptive prediction channel estimation on achievable BER performance.

where Γ is the average E_b/N_0 per antenna. It was confirmed that the BER performances with ideal channel estimation plotted in Figs. 5 and 6 agree well with the theoretical ones computed from Eq. (10).

In a slow fading channel ($f_d T_{slot} = 0.0064$), as the value of K increases, the BER performance improves. For both cases of simple averaging filter and linear interpolation filter in the 3rd step, the required E_b/N_0 for the average $BER = 10^{-3}$ can be reduced by about 0.4 dB and 0.6 dB with $K = 3$ and 4 as compared to $K = 2$. Since almost the same BER performance is observed with $K \geq 4$, we used $K = 4$ in the following simulations. In a fast fading channel ($f_d T_{slot} = 0.128$), a BER floor due to the random phase noise is observed. In such a fast fading, the use of linear interpolation filter in the 3rd step provides much smaller BER floor value.

4.3 Comparison with Conventional Non-adaptive WMSA Channel Estimation

First, we assume no frequency offset ($\delta f = 0$) and compare the average BER performances achievable with adaptive prediction channel estimation and conventional non-adaptive WMSA channel estimation. The simulated average BER performances are plotted in Fig. 6 for a slow fading channel ($f_d T_{slot} = 0.064$). When simple averaging (SA) filter is used in the 3rd step, an E_b/N_0 degradation of $K = 4$ adaptive prediction channel estimation from the ideal channel estimation case is only about 1.2 dB for achieving $BER = 10^{-3}$ with $L = 2$ MRC antenna diversity. It is slightly higher and is about 1.4 dB when linear interpolation (LI) filter is used in the 3rd step. On the other hand, a larger E_b/N_0 degradation is observed with the conventional non-adaptive WMSA channel estimation; it

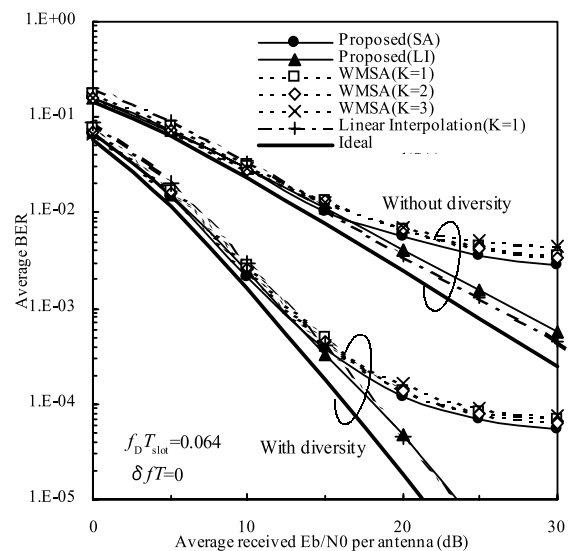


Fig. 6 Average BER performance without frequency offset.

is about 1.6 dB, 1.4 dB and 1.3 dB for $K = 1, 2$ and 3 , respectively. In the case of $K = 1$ WMSA channel estimation, the linear interpolation filter can be used; the resultant BER performance is plotted in Fig. 6 (see plots of linear interpolation ($K = 1$)). A larger E_b/N_0 degradation of 1.8 dB is observed.

The E_b/N_0 degradation of 1.2 dB for $K = 4$ adaptive prediction channel estimation is discussed below. The E_b/N_0 degradation is produced by power loss due to the transmission of non-information bearing pilot symbols, noisy channel estimate due to AWGN, and non ideal tracking of channel estimation against fast fading. For our case of $N_p = 4$ and $N_d = 60$, the power loss in dB due to pilot transmission is $\Delta p = 0.28$ dB. The E_b/N_0 degradation Δ_{SA} due to the noisy channel estimate can be computed from (see Appendix)

$$\Delta_{SA} = 10 \log_{10} \left[1 + \frac{1}{N_p} \frac{\sum_{k=-(K-1)}^K |w_{l,k}|^2}{\left| \sum_{k=-(K-1)}^K w_{l,k} \right|^2} \right] \quad (\text{dB}) \quad (11)$$

for the simple averaging filter, where $\{w_{l,k}; k = -(K-1) \sim K\}$ are elements of forward and backward predictor tap-weight vectors, $\mathbf{W}_{l,f}$ and $\mathbf{W}_{l,b}$. The converged complex tap-weights for $K = 4$ adaptive prediction channel estimation are found from computer simulation to be $\{w_{l,-3}, w_{l,-2}, w_{l,-1}, w_{l,0}, w_{l,1}, w_{l,2}, w_{l,3}, w_{l,4}\} = \{-0.09 + j0.01, 0.13 + j0.01, 0.37 + j0.02, 0.64 + j0.008, 0.63 + j0.01, 0.4 + j0.02, 0.13 + j0.02, -0.07 + j0.03\}$ for all l . Substituting these values into Eq. (11) gives $\Delta_{SA} = 0.26$ dB for our $K = 4$ adaptive prediction channel estimation. Hence, the sum of power loss due to pilot transmission and noisy channel estimate due to AWGN becomes 0.54 dB. 0.66 dB is the remaining E_b/N_0 degradation due to non ideal tracking against fast fading. On the other hand, the E_b/N_0 degradation Δ_{WMSA} due to the noisy channel estimate for conventional WMSA channel estimation can also be obtained by replacing $\{w_k\}$ in Eq. (11) with $\{w_0, w_1\} = \{1.0, 1.0\}$ for $K = 1$, $\{w_{-1}, w_0, w_1, w_2\} = \{0.6, 1.0, 1.0, 0.6\}$ for $K = 2$, and $\{w_{-2}, w_{-1}, w_0, w_1, w_2, w_3\} = \{0.3, 0.8, 1.0, 1.0, 0.8, 0.3\}$ for $K = 3$. Substituting the tap-weights into Eq. (11) gives $\Delta_{WMSA} = 0.51, 0.28$, and 0.21 dB for $K = 1, 2$, and 3 , respectively. Hence, the E_b/N_0 degradation due to non ideal tracking against fast fading becomes 0.81, 0.84, and 0.81 dB for $K = 1, 2$, and 3 , respectively. As a consequence, it can be concluded that $K = 4$ adaptive prediction channel estimation provides better tracking ability against fading than WMSA channel estimation. (Note that obtaining theoretically the E_b/N_0 degradation due to non ideal tracking against fast fading is quite difficult if not impossible and is left for a future

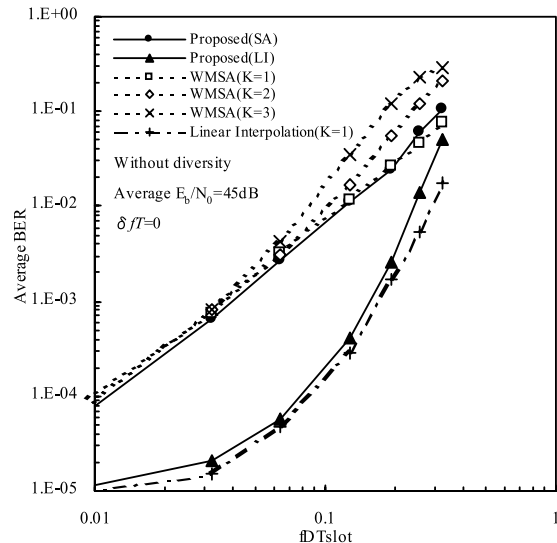


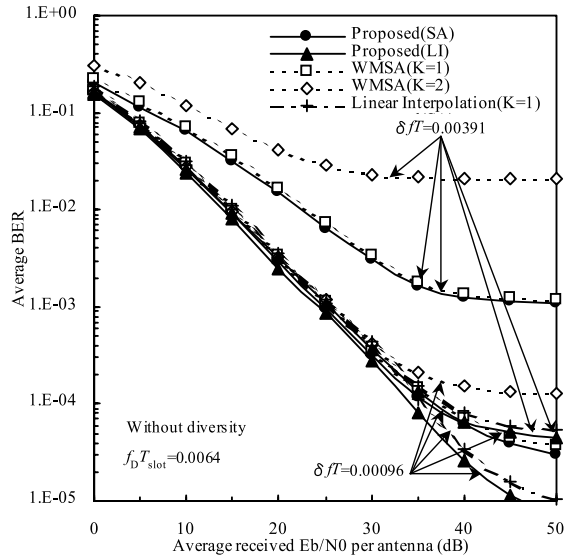
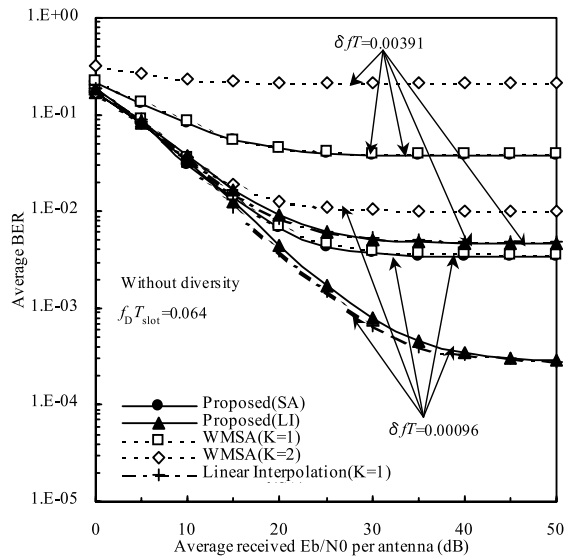
Fig. 7 BER floors in the presence of no frequency offset.

study.)

Figure 7 compares the BER floors achievable with $K = 4$ adaptive prediction channel estimation and conventional non-adaptive $K = 1-3$ WMSA channel estimation seen at the average $E_b/N_0 = 45$ dB as a function of fDT_{slot} . Also plotted are the results of simple linear interpolation ($K = 1$). For the conventional WMSA channel estimation, the BER floor becomes larger as the value of K increases, because tracking ability against fast variations in the channel gain tends to be lost, but the BER floor with adaptive prediction channel estimation using linear interpolation in the 3rd step is almost the same as that with the linear interpolation ($K = 1$).

As a consequence, the use of $K = 4$ adaptive prediction channel estimation using linear interpolation in its 3rd step can achieve almost the same BER performance as the conventional $K = 3$ WMSA in a slow fading channel, while it can achieve almost the same BER floor as the simple linear interpolation ($K = 1$) in a fast fading channel.

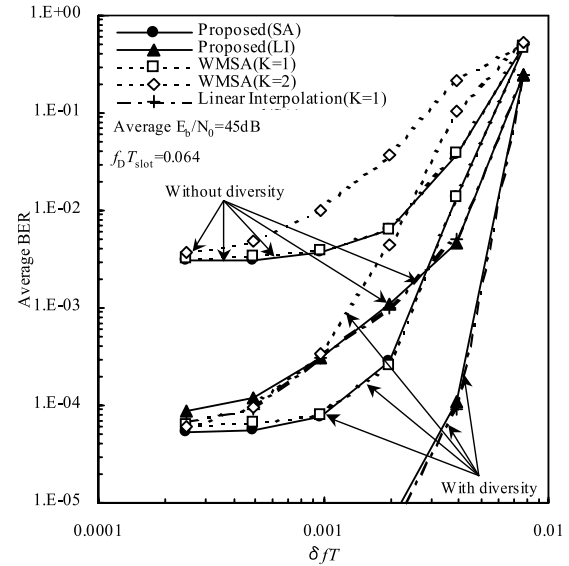
Finally, we discuss the BER performances in the presence of the frequency offset ($\delta f \neq 0$). Figure 8 plots the average BER performances with $\delta f T = 0.00096$ and 0.00391 . When the AWGN is a predominant cause of errors, i.e., in small E_b/N_0 regions, the $K = 4$ adaptive prediction channel estimation using linear interpolation in its 3rd step achieves almost the same performance as the conventional WMSA channel estimation and performs better than the linear interpolation ($K = 1$). However, when the frequency offset is a predominant cause of errors, i.e., in large E_b/N_0 regions with large frequency offset, it can achieve almost the same BER performance as the linear interpolation ($K = 1$). This can be more clearly seen in Fig. 9, which plots the BER floor as a function of $\delta f T$ at the average $E_b/N_0 = 45$ dB

(a) $f_D T_{slot} = 0.0064$ (b) $f_D T_{slot} = 0.064$ **Fig. 8** Average BER performance in the presence of frequency offset.

and $f_D T_{slot} = 0.064$.

5. Conclusion

In this paper, a pilot-aided adaptive prediction channel estimation was proposed. The tap-weights for forward prediction and backward prediction are updated using the NLMS algorithm. The BER performance using the proposed $K = 4$ adaptive prediction channel estimation was evaluated by computer simulations. The adaptive prediction channel estimation using the step size $\mu = 0.1$ and linear interpolation in its 3rd step can achieve almost the same performance as the conventional $K = 3$ WMSA in a slow fading channel, while it

**Fig. 9** BER floors in the presence of frequency offset.

can achieve almost the same BER floor as that using the simple linear interpolation ($K = 1$) in a fast fading channel and/or in the presence of frequency offset. The proposed adaptive prediction channel estimation can also be applied to DS-CDMA coherent rake reception in a frequency selective fading channel.

References

- [1] W.C., Jakes Jr., ed., *Microwave Mobile Communications*, Wiley, New York, 1974.
- [2] S. Sampei and T. Sunaga, "Rayleigh fading compensation for QAM in land mobile radio communications," *IEEE Trans. Veh. Technol.*, vol.42, no.2, pp.137-147, May 1993.
- [3] F. Ling, "Coherent detection with reference-symbol based estimation for direct sequence CDMA uplink communications," *Proc. IEEE Vehicular Technol. Conference*, New Jersey, pp.400-403, May 1993.
- [4] C.I. Bang and M.H. Lee, "An analysis of pilot symbol assisted 16QAM in the Rayleigh fading channel," *IEEE Trans. Consum. Elect.*, vol.41, no.4, pp.1138-1141, Nov. 1995.
- [5] H. Andoh, M. Sawahashi, and F. Adachi, "Channel estimation filter using time-multiplexed pilot channel for coherent rake combining in DS-CDMA mobile radio," *IEICE Trans. Commun.*, vol.E81-B, no.7, pp.1517-1526, July 1998.
- [6] Y. Honda and K. Jamal, "Channel estimation based on time-multiplexed pilot symbols," *IEICE Technical Report*, RCS96-70, Aug. 1996.
- [7] M. Shimizu, K. Matsuyama, T. Dateki, H. Furukawa, and Y. Tazawa, "Pilot symbol assisted channel estimation with wiener filtering for DS-CDMA," *Proc. 3rd Inter. Symp. of MDMC'98*, California, U.S.A, pp.86-90, Sept. 1998.
- [8] S. Abeta, M. Sawahashi, and F. Adachi, "Adaptive channel estimation for coherent DS-CDMA mobile radio using time-multiplexing pilot and parallel pilot structures," *IEICE Trans. Commun.*, vol.E82-B, no.9, pp.1505-1513, Sept. 1999.
- [9] K. Hamaguchi, "A frequency offset compensation method for received QAM signal in land mobile communications," *IEICE Trans. Commun. (Japanese Edition)*, vol.J79-B-II, no.7, pp.426-428, July 1996.

- [10] S. Haykin, Adaptive filter theory, 3rd edition, Prentice Hall, 1996.
 [11] J.G. Proakis, Digital Communications, 3rd ed., McGraw Hill, New York, 1995.

Appendix: Obtaining Eq. (11)

The E_b/N_0 degradation due to the noisy channel estimate is theoretically derived, assuming no frequency offset $\delta f = 0$, for the simple averaging filter. The first step coherently adds the N_p received pilot symbols to obtain the instantaneous channel estimate $\hat{\xi}_l(m)$ at the beginning of the m th data slot. $\hat{\xi}_l(m)$ may be expressed as

$$\hat{\xi}_l(m) = \sqrt{2S}\xi_l(m) + \hat{\rho}_l(m), \quad (\text{A}\cdot 1)$$

where $\hat{\rho}_l(m)$ is the noise component, due to AWGN, with zero mean and a variance of $(2N_0/T)N_p$. Then, the second step predicts the instantaneous channel gains, $\tilde{\xi}_{l,f}(m)$ and $\tilde{\xi}_{l,b}(m)$, at the end and the beginning of the m th data slot, by a forward predictor and a backward predictor, using the K past and K future estimated instantaneous channel gains, $\{\hat{\xi}_l(m+k)\}$, $k = -(K-1) \sim K$, respectively, as shown in Eqs. (6a) and (7a). Assuming the simple averaging filter, the third step estimates the instantaneous channel gain $\tilde{\xi}_l(m,n)$ at the n th data symbol position of the m th data slot by simply summing the two adaptively predicted instantaneous channel gains, $\tilde{\xi}_{l,f}(m)$ and $\tilde{\xi}_{l,b}(m)$. From Eqs. (A.1), (6), and (8a), $\tilde{\xi}_l(m,n)$ may be expressed as

$$\begin{aligned} \tilde{\xi}_l(m,n) &= \frac{1}{2}[\tilde{\xi}_{l,f}(m) + \tilde{\xi}_{l,b}(m)] \\ &= \frac{1}{2} \sum_{k=-(K-1)}^K w_{l,k}(m) \hat{\xi}_l(m+k) \\ &= \frac{1}{2} \sum_{k=-(K-1)}^K w_{l,k}(m) \{\sqrt{2S}\xi_l(m+k) + \hat{\rho}_l(m+k)\}. \end{aligned} \quad (\text{A}\cdot 2)$$

Assuming a very slow fading such that the channel gain remains constant over a period of at least $2K$ slots, i.e., $\xi_l(m+k) \approx \xi_l(m)$ for $k = -(K-1) \sim K$, Eq. (A.2) becomes

$$\tilde{\xi}_l(m,n) \approx \alpha_l \{\sqrt{2S}\xi_l(m) + \tilde{\rho}_l(m)\}, \quad (\text{A}\cdot 3)$$

where $\alpha_l = \frac{1}{2} \sum_{k=-(K-1)}^K w_{l,k}(m)$ and $\tilde{\rho}_l(m)$ is the noise component with zero mean and a variance of

$$\sigma_\rho^2 = \frac{2N_0}{T} \frac{1}{N_p} \frac{\sum_{k=-(K-1)}^K |w_{l,k}(m)|^2}{\left| \sum_{k=-(K-1)}^K w_{l,k}(m) \right|^2}. \quad (\text{A}\cdot 4)$$

Using the noisy channel estimate, coherent detection is performed. The MRC combiner output $\tilde{d}(m,n)$ of Eq. (4) is expressed as

$$\begin{aligned} \tilde{d}(m,n) &= \sum_{l=1}^L r_l(m,n) \tilde{\xi}_l^*(m,n) \\ &\approx \sum_{l=1}^L \{\sqrt{2S}d(m,n)\xi_l(m) + \rho_l(m,n)\} \\ &\quad \times \alpha_l \{\sqrt{2S}\xi_l(m) + \tilde{\rho}_l(m)\}^* \\ &\approx \sum_{l=1}^L \alpha_l \{\sqrt{2S}d(m,n)\xi_l(m) + \eta_l(m,n)\} \\ &\quad \times \sqrt{2S}\xi_l^*(m) \end{aligned} \quad (\text{A}\cdot 5)$$

for a large E_b/N_0 , where $\eta_l(m,n) = \rho_l(m,n) + \tilde{\rho}_l(m)d(m,n)$ is the equivalent noise component with zero mean and a variance of

$$\sigma_\eta^2 = \frac{2N_0}{T} \left(1 + \frac{1}{N_p} \frac{\sum_{k=-(K-1)}^K |w_{l,k}(m)|^2}{\left| \sum_{k=-(K-1)}^K w_{l,k}(m) \right|^2} \right). \quad (\text{A}\cdot 6)$$

Note that the value of σ_η^2 is the same for all l when the tap-weights converge. For ideal channel estimation, $\tilde{\rho}_l(m) = 0$. Hence, the E_b/N_0 degradation Δ_{SA} due to the noisy channel estimate is given by

$$\Delta_{SA} = 10 \log_{10} \left[1 + \frac{1}{N_p} \frac{\sum_{k=-(K-1)}^K |w_{l,k}(m)|^2}{\left| \sum_{k=-(K-1)}^K w_{l,k}(m) \right|^2} \right] \quad (\text{dB}) \quad (\text{A}\cdot 7)$$

for the simple averaging filter.



Shinsuke Takaoka received his B.S. degree in communications engineering from Tohoku University, Sendai, Japan, in 2001. Currently, he is a graduate student at the Department of Electrical and Communications Engineering, Tohoku University. His research interests include wireless digital signal transmission techniques, especially for mobile communications systems.



Fumiyuki Adachi received his B.S. and Dr.Eng. degrees in electrical engineering from Tohoku University, Sendai, Japan, in 1973 and 1984, respectively. In April 1973, he joined the Electrical Communications Laboratories of Nippon Telegraph & Telephone Corporation (now NTT) and conducted various types of research related to digital cellular mobile communications. From July 1992 to December 1999, he was with NTT Mobile

Communications Network, Inc. (now NTT DoCoMo, Inc.), where he led a research group on wideband/broadband CDMA wireless access for IMT-2000 and beyond. Since January 2000, he has been with Tohoku University, Sendai, Japan, where he is a Professor of Electrical and Communication Engineering at Graduate School of Engineering. His research interests are in CDMA and TDMA wireless access techniques, CDMA spreading code design, Rake receiver, transmit/receive antenna diversity, adaptive antenna array, bandwidth-efficient digital modulation, and channel coding, with particular application to broadband wireless communications systems. From October 1984 to September 1985, he was a United Kingdom SERC Visiting Research Fellow in the Department of Electrical Engineering and Electronics at Liverpool University. From April 1997 to March 2000, he was a visiting Professor at Nara Institute of Science and Technology, Japan. He was a co-recipient of the IEICE Transactions best paper of the year award 1996 and again 1998. He is an IEEE Fellow and was a co-recipient of the IEEE Vehicular Technology Transactions best paper of the year award 1980 and again 1990 and also a recipient of Avant Garde award 2000.